LUND UNIVERSITY

Understanding the characteristics of non-equilibrium alternating current gliding arc discharge in a variety of gas mixtures (air, N_2, Ar, Ar/O_2, and Ar/CH_4) at elevated pressures (1-5 atm)

Kong, Chengdong; Gao, Jinlong; Ehn, Andreas; Aldén, Marcus; Li, Zhongshan

Creative Commons License:
CC BY

LUND UNIVERSITY

PO Box 117
221 00 Lund
+46 46-222 00 00

Understanding the characteristics of non-equilibrium alternating current gliding arc discharge in a variety of gas mixtures (air, N₂, Ar, Ar/O₂, and Ar/CH₄) at elevated pressures (1–5 atm)

Chengdong Kong, Jinlong Gao, Andreas Ehn, et al.

View Online   Export Citation   CrossMark

ARTICLES YOU MAY BE INTERESTED IN

Influence of high energy electrons on negative ion density in a hot cathode discharge
Physics of Plasmas 29, 033501 (2022); https://doi.org/10.1063/5.0078194

Effect of electron density gradient on power absorption during gigahertz electromagnetic wave propagating in cold plasma
Physics of Plasmas 29, 033301 (2022); https://doi.org/10.1063/5.0080079

Toward the core-edge coupling of delta-f and total-f gyrokinetic models
Physics of Plasmas 29, 032301 (2022); https://doi.org/10.1063/5.0077557

Understanding the characteristics of non-equilibrium alternating current gliding arc discharge in a variety of gas mixtures (air, N₂, Ar, Ar/O₂, and Ar/CH₄) at elevated pressures (1–5 atm)

Chengdong Kong,[1,2,a] (iD) Jinlong Gao,[2] (iD) Andreas Ehn,[2] (iD) Marcus Aldén,[2] and Zhongshan Li[2] (iD)

AFFILIATIONS

[1]Institute of Thermal Energy Engineering, School of Mechanical Engineering, Shanghai Jiao Tong University, Shanghai 200240, China
[2]Division of Combustion Physics, Lund University, P.O. Box 118, S-221 00 Lund, Sweden

[a]Author to whom correspondence should be addressed: kongcd19@sjtu.edu.cn

ABSTRACT

This work aims at clarifying the fundamental mechanisms of non-equilibrium alternating current gliding arc discharge (GAD) by investigating effects of gas compositions and pressures on the GAD characteristics with electrical and optical methods. Interestingly, the glow-to-spark transition was found by adding O_2 or CH_4 into the argon or modulating the power supply. This transition occurs attributed to the fact that the discharge mode is largely affected by the effective electron decay time (τ) as well as the feedback response of the power supply to the free electron density in the GAD. Short τ or low free electron density tends to result in the spark-type discharge. It further implies that the power supply characteristics is crucial for discharge mode control. The pressure effects on the GAD characteristics were found to vary with gas composition when the same alternating current power supply was used. In N_2 or air, the emission intensity from the plasma column increases with pressure while the mean electric field strength (E) along the plasma column decreases with pressure. Differently, in Ar, the emission intensity and E do not change much with pressure. It can be explained by the different energy partition and transfer pathways between monatomic and molecular species. The molecular gases have vibrational excitation pathways to facilitate the electronic excitation and ionization that is different from the monatomic gas.

Published under an exclusive license by AIP Publishing. https://doi.org/10.1063/5.0066952

I. INTRODUCTION

Gliding arc discharge (GAD), which occurs when the plasma is generated between two or more diverging electrodes placed in a fast gas flow,[1] has been proposed for many decades.[2] In 1999, a review paper of GAD was reported by Fridman *et al.*[1] It was pointed out that the GA has transitions from equilibrium phase to non-equilibrium phase. The physical parameters of the equilibrium phase of the gliding arc evolution are similar to those for regular, high pressure (p > 0.1–0.5 atm) arc discharges, which have features of high values of current (1–10⁵A) and rather low values of voltage.[1] The equilibrium phase of gliding arc discharge can provide sufficient power levels but are not adapted to the purposes of plasma chemistry. In the recent decade, the non-equilibrium GAD becomes of increasing interest for applications and is widely explored. In fact, when the input power is limited to be less than 0.5 kW, a warm and non-equilibrium plasma, which has a relatively high gas temperature of 1000–4000 K and an electron temperature of 1–3 eV,[3–5] can be easily produced during the GAD. This kind of plasma has been termed as "warm plasma" by more and more scholars.[6–8] Owing to its combined thermal and chemical effects, as well as its easy handling at the atmospheric pressure, the non-equilibrium gliding arc discharge (NE-GAD) is a very promising technique for applications in energy and environmental fields, such as plasma assisted combustion,[9,10] plasma reforming,[11] and pollutant treatment.[12,13]

Toward high energy and conversion efficiencies in the aforementioned applications, the NE-GAD characteristics, including the discharge modes and the apparent morphologies, in given reacting systems should be comprehensively understood. The discharge mode of NE-GAD has been investigated under different flow conditions.[14–17]

Two discharge modes, i.e., glow-type discharge and spark-type discharge,[17,18] are categorized. The glow-type discharge denotes the plasma filament with current value less than 1 A and a cathode fall of 300–500 V.[18] The spark-type discharge is characterized by a bright plasma filament with current spikes, which are alternate rapidly. Usually, in a jet flow, with the jet flow rate increase, the discharge can undergo the glow-to-spark transition, attributed to the turbulence-promoted dissipations of energy and radicals around the plasma column.[17] Here, the glow-to-spark transition denotes the transition from the glow-type discharge to the repetitive spark-type discharges. The control of glow-to-spark transition in NE-GAD is vital in the practice but the underlying mechanism is not scrutinized yet, needing more investigation.

The dynamical morphology of the produced plasma in the NE-GAD was extensively studied by using high-speed photography. The conventional GAD using two diverging plates as electrodes usually looks planar, but the GA can also move rotationally in the swirling flow[19–21] by using specially designed electrodes. Essentially, the planar or rotating GADs are similar since their transient morphologies can both be represented by a curved filamentary plasma column.[14,16] However, the dynamical trajectory of the plasma column varies depending on the flow field,[16,17] the magnetic field,[4,22,23] and the gravity field[24,25] through the drag force, the Lorentz force, and the buoyancy force, respectively. To control the dynamical morphologies of gliding arc, the design of electrode configurations is a direct way by regulating the flow field or electric field and, thereby, influencing the propagation behaviors of gliding arc. Up to now, different electrode configurations, such as bended tubes,[17] coaxial electrodes,[21] two-ring electrodes,[26] and three diverging planar electrodes,[27] have been reported to form various rotating or planar NE-GADs.

Summarily, the characteristics of NE-GAD can be influenced by many factors, including gas flow rate, gravity, magnetic field, electrode configuration, gas composition, gas temperature, pressure, and power supply. However, those factors are not easy to be systematically explored. Up to now, the flow rate effect has been explored in detail due to its easy regulation, but the influences of many other factors on NE-GAD are seldomly studied. For example, different electrode configurations were utilized and characterized but the dependence on electrode configurations by using the same power supply was rarely explored. Similarly, a large number of gaseous mixtures have been used for different applying purposes but the comparison was not often reported. To the best of our knowledge, only Roy *et al.*[28] studied the gas-dependent structures and properties of GAD in Ar, O_2, and air recently. Since the setup configuration and the used power supply can both impact the discharge characteristics, it is necessary to study the isolated effects of gas composition on NE-GAD by using the same electrodes and the same power supply. Otherwise, the discrepancies may be difficult to explain. The pressure effect above the atmospheric pressure on the GAD was usually explored when the current was quite large (>50 A). For instance, Rutberg *et al.* found that the voltage dropped on the arc increased with pressure from 0.2 to 2 MPa at currents 250–380 A in the nitrogen flow.[29] However, for the NE-GAD with relatively low current less than 1 A, the pressure effect above the atmospheric pressure is not explored yet, to our knowledge. Even though the atmospheric pressure is convenient for most applications, but for special applications, such as the gas turbine combustion, the high-pressure non-thermal discharge study is necessary if the

NE-GAD is used for flame stabilization. Therefore, the pressure dependence of NE-GAD above the atmospheric pressure needs exploration.

Aiming at clarifying the glow-to-spark transition and the gas-dependent pressure effect on the NE-GAD characteristics, this work investigates the effects of gas compositions on the GAD characteristics (including the electrical properties, the discharge mode, and the morphologies of GAD) at elevated pressures from 1 to 5 atm by collecting the current–voltage (I–U) waveforms and the discharge images. A simplified mechanism is further proposed to explain the properties of NE-GAD in various gas mixtures at elevated pressures up to 5 atm.

II. EXPERIMENTAL SETUP

The experimental setup has been used in the previous work[30] and is thereby described in brief here. Figure 1 shows a schematic of the experimental apparatus. A pair of diverging electrodes made of stainless steel to support the gliding arc discharge was installed on a Teflon plate inside a high-pressure chamber. The high-pressure chamber was originally used for a combustion study, and details are reported in Ref. 31. One of the electrodes was connected to an AC power supply (Generator 9030 E, SOFTAL Electronic GmbH) through an insulated connector on the wall of the chamber, whereas the other electrode and the metal chamber were both grounded. The frequency of the alternating current power supply is 35 kHz. Various gas mixtures, including air, N_2, Ar, Ar/O_2, and Ar/CH_4, were separately ejected into the chamber through a small hole (3 mm) between the electrodes on the Teflon plate. The mass flow rates were controlled by high-pressure mass flow controllers (Brooks Instruments, SLA5850S) to be 10 standard liter per minute (SLPM) in total and fixed even though the pressure changed from 1 to 5 atm. The pressure in the chamber was controlled by regulating the flow of exit gas using electronic operated back-pressure regulators. Three broadband anti-reflection coated sapphire windows provide optical access for the GAD inside the chamber. Optical equipment, including a digital camera (D7100, Nikon) equipped with micro-Nikon lens (200 mm, f/4), an intensified charged-coupled device (ICCD, PIMAX II, Princeton Instruments) mounted with a UV Nikon lens (105 mm, f/4.5), a spectrometer (SP 2300i, Princeton Instruments), and a high-speed camera (Phantom 7.2, Vision Research), was employed to characterize the NE-GAD in different gas mixtures. A current monitor (Pearson 6585) and a voltage probe (Tektronix P6015A) were put inside the chamber and utilized to measure the waveforms of the current and the voltage simultaneously. The current and voltage waveforms were recorded by a four-channel oscilloscope (PicoScope 4424).

III. RESULTS
A. Definition of discharge modes of GAD in AC electric field

Since the glow-type GAD, the spark-type GAD, and the glow-to-spark transition in an AC electric field are to be investigated in Secs. III B and III C, they are first defined and clarified. Here, a glow-type discharge is characterized by relatively low current (<1 A) and fairly high voltage (>1 kV) with a cathode fall of 300–500 V.[18] More importantly, for a quasi-steady glow-type discharge in an alternating electric field, the current follows the alternating voltage well without any spikes. The typical current and voltage waveforms of glow-type discharge can be found in Fig. 2(a). A spark-type discharge is a transient phenomenon characterized by a suddenly brightened discharge
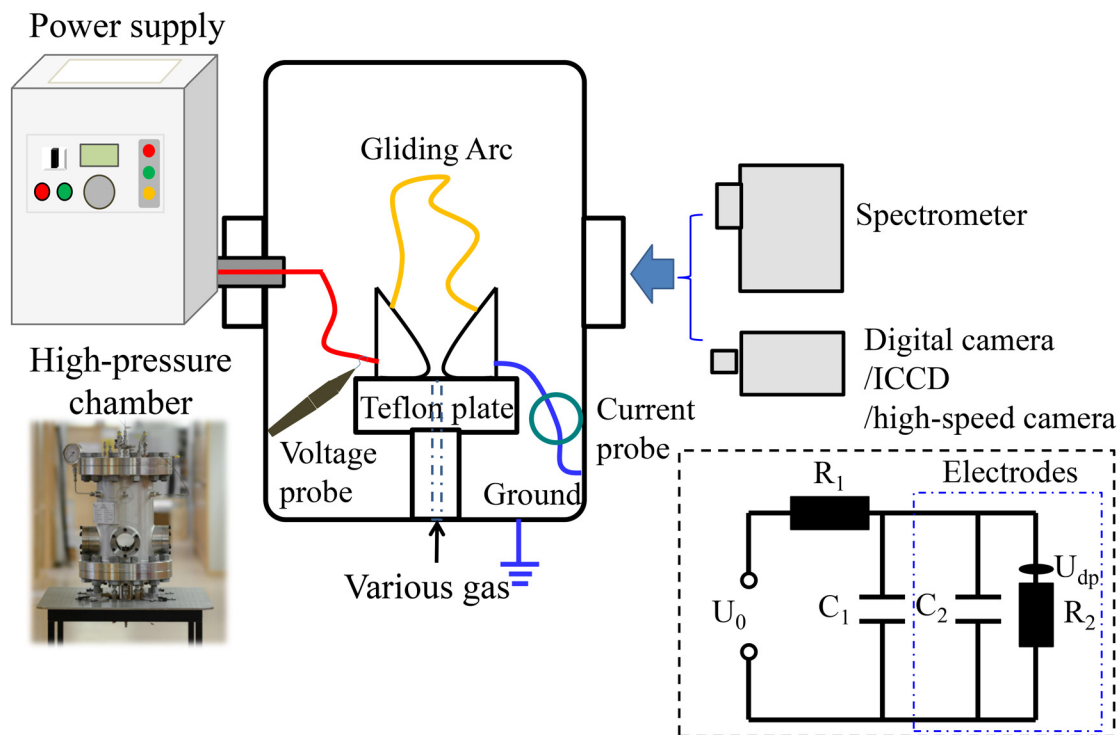
FIG. 1. Schematic of the experimental setup. The equivalent electrical circuit of the discharge system is plotted in the dashed box. R_1 and C_1 represent the equivalent resistance and capacitance of the coaxial cable. C_2 represents the equivalent capacitance of the electrodes, and R_2 is the resistance of produced plasma. U_{dp} represents the effective voltage drop near the electrodes during the glow-type discharge.

channel and current spikes whose peak value is much larger than 1 A. Its typical current and voltage waveforms can be found in Fig. 2(b). The full width at half maximum (FWHM) of the current spike should be less than hundreds of nanoseconds. The spark-type discharge occurs due to the gas breakdown developing with rapid growth of plasma channel from one electrode to another. It should be stressed that the spark discharge can take place in either the cold, non-ionized gas or the warm, weakly ionized plasma column. Since their local environment can be completely different, the electric field strength of

breakdown varies. In this work, the spark-type discharge refers in particular, to the breakdown in the warm, weakly ionized plasma channel, whose electric field strength of breakdown is termed as E_{sp}. The current waveforms of the glow-type and the spark-type discharges are clearly different, so the current waveforms can be used to distinguish the glow-type or the spark-type discharge. Furthermore, because the spark-type discharge is a transient phenomenon while the glow-type discharge can be treated as a quasi-steady phenomenon, they are not directly comparable and it is not easy to define the glow-to-spark
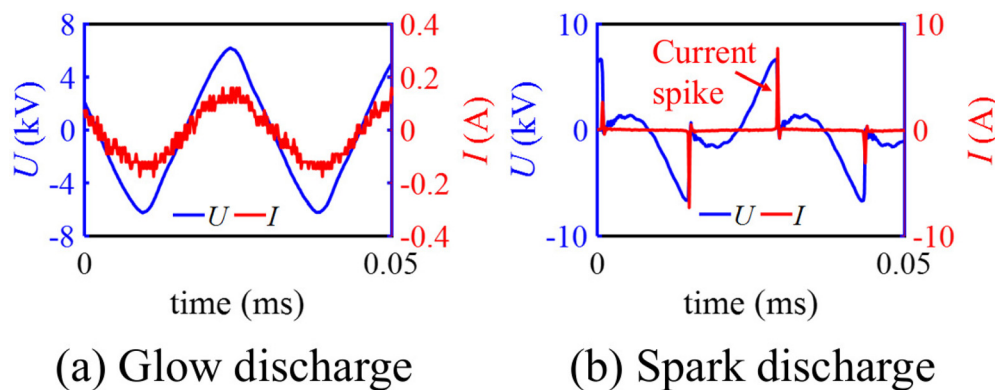
FIG. 2. Typical current (I) and voltage (U) waveforms of (a) a glow-type discharge and (b) a spark-type discharge.
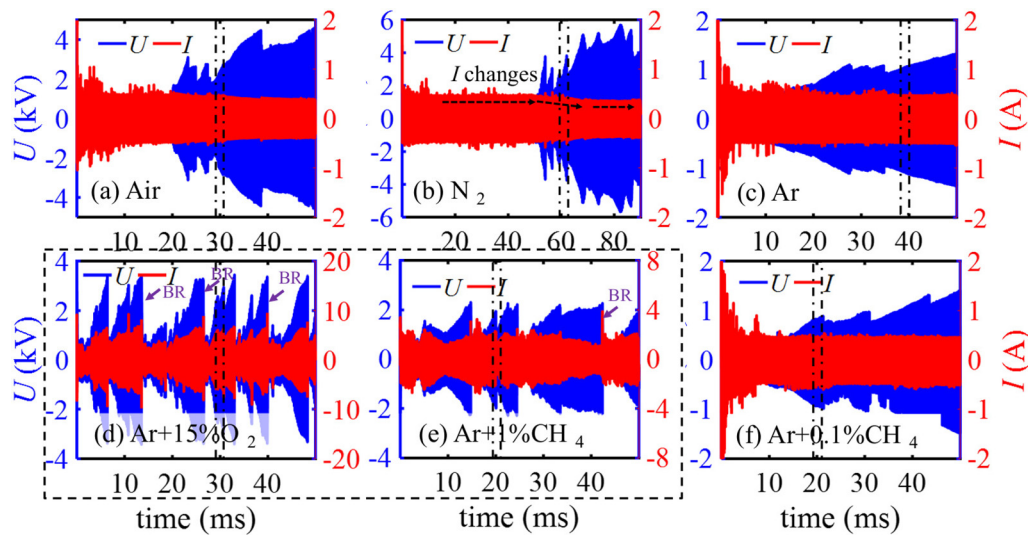
FIG. 3. Current (I) and voltage (U) waveforms of GAD in different gas mixture. The dashed box marks two cases with the spark discharge. BR: Breakdown Reignition over the shortest gap between electrodes. The dash-dotted lines indicate the range of waveforms, which are zoomed in and replotted in Fig. 4.

transition. However, the repetitive spark-type discharges can be regarded as a quasi-steady discharge state and, thereby, the glow-to-spark transition in this work denotes the transition from the quasi-steady glow discharge state to the repetitive spark discharge state.

B. Effects of gas compositions on the NE-GAD characteristics

1. Gas-dependent electrical properties of NE-GAD

Figure 3 demonstrates the current (I) and voltage (U) waveforms of GAD in different gaseous mixtures (i.e., air, N_2, Ar, Ar/O_2, and Ar/CH_4)

at the atmospheric pressure. Figure 4 shows the corresponding zoomed-in I–U waveforms within given time windows of Fig. 3. It is found that in air, N_2, and Ar, the waveforms of current and voltage are nearly sinusoidal and the phase shift between I and U is negligible, implying that the plasma column can be regarded as a conductive load. Furthermore, after the initial breakdown, the current amplitude is less than 1 A without current spikes, which means a glow-type discharge in air, N_2 or Ar. For the glow-type GAD, the voltage amplitude increases with the elongation of the plasma column. Nevertheless, when the plasma column is long enough, it can be stretched and distorted by the eddy flow to arise new high-conductivity channel (called as short-cutting events[16]).
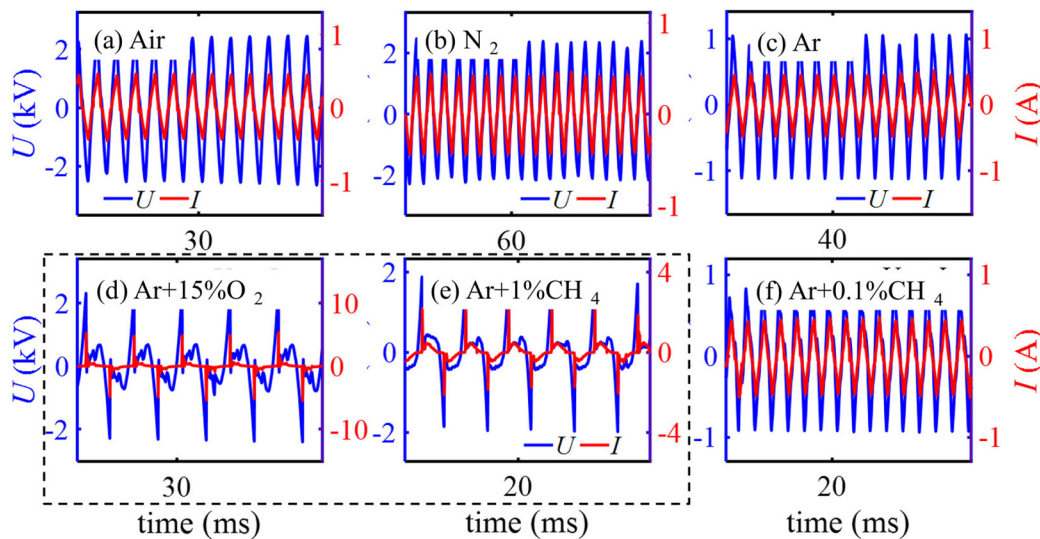
FIG. 4. Zoomed-in I–U waveforms of GAD within a narrow time window, corresponding to Fig. 3.

This event limits the maximum length of the plasma channel and also contributes to the saw-toothed shapes of voltage envelope. Compared to the voltage amplitude, the current amplitude changes slightly with the plasma elongation. When the voltage amplitude is less than 1.5 kV, the current amplitude is saturated to be 0.5 A. When the voltage is higher than 1.5 kV, the current amplitude decreases with the further increment of voltage [marked in Fig. 3(b)]. This negative correlation between voltage and current can be ascribed to the fact that the rated power, which are time-averaged product of the voltage and the current, is limited by the power supply.

Even though the GAD in air, N_2, and Ar is all glow-type discharges with similar I-U waveforms, the absolute values are distinct. The measured voltage amplitude of GAD in Ar is less than 1.5 kV and much lower than that in air or N_2. As a result, the current amplitude is stabilized at 0.5 A in Ar. Moreover, due to the small voltage amplitude, the breakdown over the shortest gap between electrodes occurs scarcely and the plasma column can be much longer than 20 cm in Ar.

Interestingly, with the addition of O_2 or CH_4 in Ar, the electrical characteristics change greatly, according to the I–U waveforms in Figs. 3 and 4. As an example shown in Fig. 4(d), with 15% of O_2 mixed in argon, the current spikes with peak values larger than 1 A appear repetitively that manifests a spark-type discharge and, thereby, confirms a glow-to-spark transition with the addition of O_2 in pure argon. Moreover, the growth rate of the voltage amplitude in the Ar–O_2 mixture is larger than that in the pure Ar and the peak voltage can reach the threshold of breakdown over the shortest gap between electrodes, marked as BR in Fig. 3(d). For the spark-type discharge, the current spike value grows with the voltage amplitude that is opposite to that for the glow-type discharge. It is possibly explained by that with the plasma elongation, the voltage for spark discharge increases and the resulted displacement current during spark discharge grows to elevate the spike current value.

To explain the glow-to-spark transition as O_2 is added in Ar, we assume a scenario that initially the GAD occurs in the pure argon and later the oxygen is mixed. The molecular O_2 can attach electrons efficiently to reduce the electron concentration. As the electron concentration decreases, the current and the power both decline. The power supply has a feedback response to keep the output power, so the voltage increases, in order to maintain the rated power. When the voltage reaches a critical value, breakdown along the plasma column (the so-called sparks in this work) occurs, accompanied by current spikes.

2. Gas-dependent morphologies of plasma in NE-GAD

The morphologies of the plasma column of GAD in different gas mixtures have been captured by a Nikon digital camera with an exposure time of 1/8000 s, as shown in Fig. 5. The shape and the color of the plasma columns vary distinctly with gas types. The colorful plasma columns are because of the production of different excited species. To gain insights into these excited species, an ICCD camera (Princeton Pi-Max II) was mounted on a spectrometer (SP 2300i, Princeton Instruments) to acquire the spectra with a single-shot gate time of 0.5 ms. The wavelength was scanned from 300 to 500 nm, and the typical emission spectra in the waveband from 330 to 450 nm are displayed in Fig. 6. It indicates that in air, the emission is mainly from NO (B-X) transitions. The N_2(C-B) emission has been hardly detected for the glow-type air discharge, while for the spark-type discharge, the
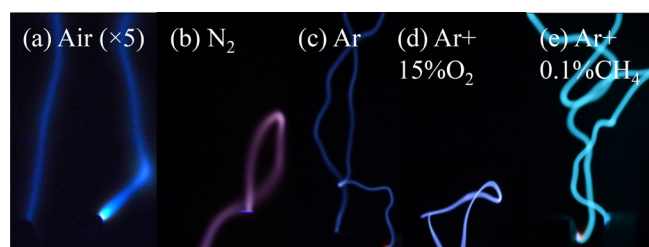

FIG. 5. Morphologies of plasma columns in different gas mixtures captured by a Nikon digital camera.

N_2(C-B) emission dominates since the N_2(C) can only be efficiently produced by electron impact excitation in air. In the pure N_2, the emissions from the N_2(C-B) transitions and the ionic N_2^+(B-X) transitions are detected. In Ar, some specific peaks from the atomic Ar have been detected but the spectral resolution is too low to distinguish each transition lines in the current work. In the Ar/15%O_2 mixture, the continuous spectrum is much stronger and the peaks around 330 nm become much weaker compared to the spectra in Ar.

According to Fig. 5, the plasma column looks diffusive in air and N_2. The estimated diameter is around 1.5 mm. The maximum length of the plasma column is less than 10 cm. The plasma channel looks smooth without many curved or twisted shapes, whereas, in Ar, the plasma column looks thinner with an estimated diameter of around 0.44 mm. The plasma column can be elongated to be more than 20 cm. Furthermore, the plasma column is easily distorted and twisted by small vortexes in the jet flow, to result in more curved and waved shapes in Ar (see Fig. 7). The waved shape reflects the interactions between plasma and small vortexes. When the plasma column is thin, it is easy to follow the small vortexes and, thus, the plasma column can look waved. With the addition of O_2 in Ar to produce the spark-type GAD, the maximum length becomes much shorter due to the increased voltage and the plasma column becomes less curved (see Fig. 5).

With the addition of CH_4 in Ar, the repetitive current spikes are also detected when the CH_4 volume fraction reaches 1% [see Fig. 4(e)]. If the CH_4 volume fraction in Ar is less than 0.1%, the discharge is still in the glow type but the emission intensity in the waveband of 420 ± 10 nm increases by about three folds, which is similar to that found in the CH_4/N_2 mixture.[30] Additionally, the width of the bluish plasma column detected by using the interference filter with a waveband of 420 ± 10 nm is smaller than that with a waveband of 515 ± 10 nm, as shown in Figs. 8(a) and 8(b). The images captured by the Nikon digital camera also confirm that the bluish signal locates inside the greenish emission signal [see Figs. 8(c) and 8(d)]. The bluish emission is mainly from Ar related species while the greenish emission should be from the excited CH. It infers that around the plasma column, the methane can be decomposed into radicals like CH and H.

As the plasma column moves with flow, the plasma states change dynamically. By utilizing a high-speed camera, whose exposure time was 5 μs and the frame rate was 10 kHz, the emission intensity of the plasma column with respect to time is obtained, as shown in Fig. 9. Initially, the emission is intensive due to the violent breakdown process. As the plasma column elongates, the intensity drops gradually in air and N_2. Differently, in Ar, the intensity fluctuates periodically.
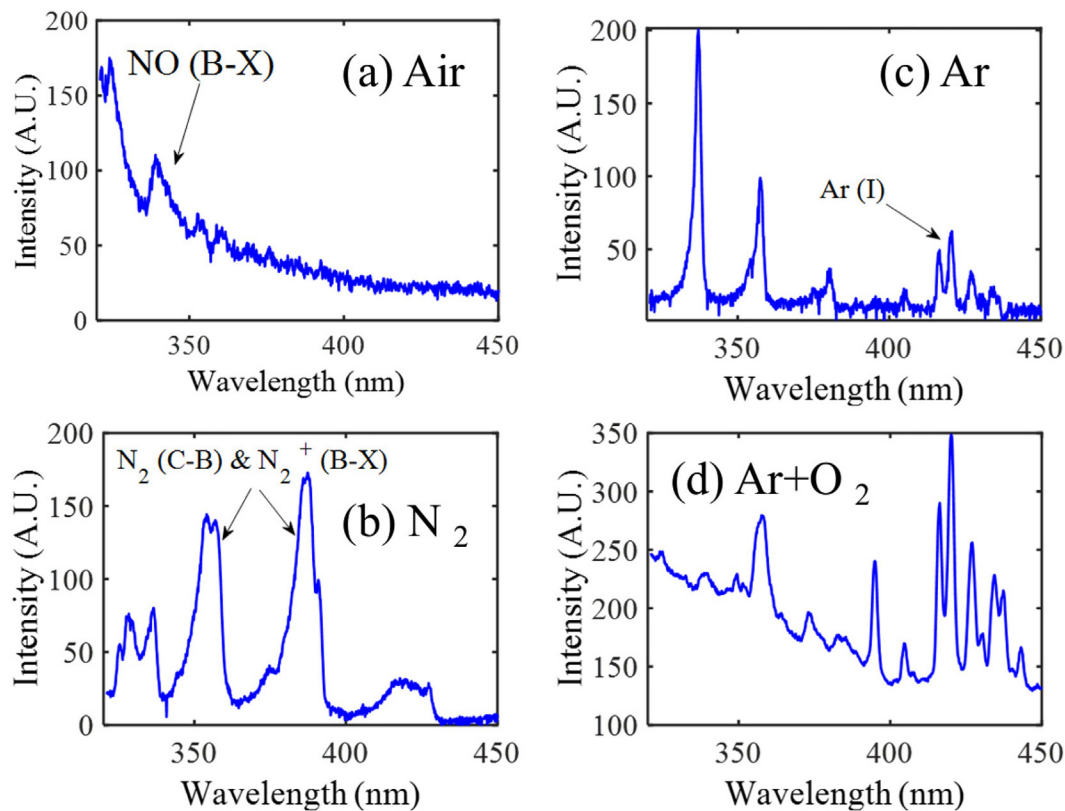
FIG. 6. Emission spectra of GAD in the waveband from 330 to 450 nm. (a) Air, (b) N_2, (c) Ar, and (d) Ar + 15% O_2.

The fluctuation of emission intensity in Ar plasma is because of the alternating voltage. High voltage is necessary to excite Ar for spontaneous emissions. It, thus, implies that the fluctuation frequency of emissions is consistent with the alternating frequency of voltage. However, since the frame rate of the high-speed camera is only 10 kHz, lower than the voltage alternating frequency (70 kHz), the captured frequency of emission fluctuation ($\sim$1.5 kHz) is much lower than the real value.

Using the simultaneously collected high-speed images and the voltage waveforms, the curves of plasma length and voltage amplitude can be plotted to derive the average electric field strength (E) along the plasma column. In Ar, this value is less than 10 kV/m, while in N_2 and air, it is much larger than 40 kV/m. A smaller E in Ar means that the plasma column is easier to be self-sustained compared to the N_2 or air plasma.

C. Gas-dependent pressure effect on the NE-GAD characteristics

The elevated pressure impacts the breakdown voltage following the Paschen's law as well as the propagation characteristics of GAD. This section focuses on the complex propagation characteristics.

Figure 10 shows the I–U waveforms of GAD in air, N_2, and Ar at the pressures of 1 and 5 atm. The GAD remains in the glow type as the pressure increases from 1 to 5 atm, but some minor differences emerge. For instance, the envelope of the voltage waveform becomes

smooth with less sawtooth features at higher pressure. It is possibly attributed to the fact that at a fixed mass flow rate, the gas velocity is lower and the flow is more laminar as the pressure increases. In addition, the current envelope has less spikes at higher pressure. Figure 11 demonstrates the emission intensity of the plasma column with respect to pressure in air, N_2, and Ar, respectively, and Fig. 12 displays the corresponding images at 1 and 5 atm. The images were captured by the ICCD camera mounted with a UV lens using a gate time of 15 μs. In air and N_2, the emission intensities increase almost linearly with pressure. The spectral analysis has indicated that the emission in N_2 is mainly from N_2^+(B–X), N_2(C–B), and N_2(B–A), while the emission in air is mainly due to the NO(B–X) transition and O_2 Schumann–Runge (B–X) transition,[32] instead of the N_2(C–B) transition (see Fig. 6). The increased emission intensities at elevated pressures imply the growing concentrations of those species and also electrons in N_2 and air, whereas, in Ar, the emission intensity is nearly constant with pressure increase. The detected intensity value has larger error bars than that in N_2 and air, since the ICCD gate is not phase matching with the fluctuating emission intensity of plasma in Ar.

Figure 13 shows the voltage amplitude-plasma length curves of the GAD in air, N_2, and Ar at pressures of 1, 3, and 5 atm. The slopes can be used to derive the electric field strength (E). In air and N_2, the E is similar and decreases with the pressure increase. The aforementioned analysis of the emission intensity infers that the electron density has increased with pressure, and thereby, the electric field strength
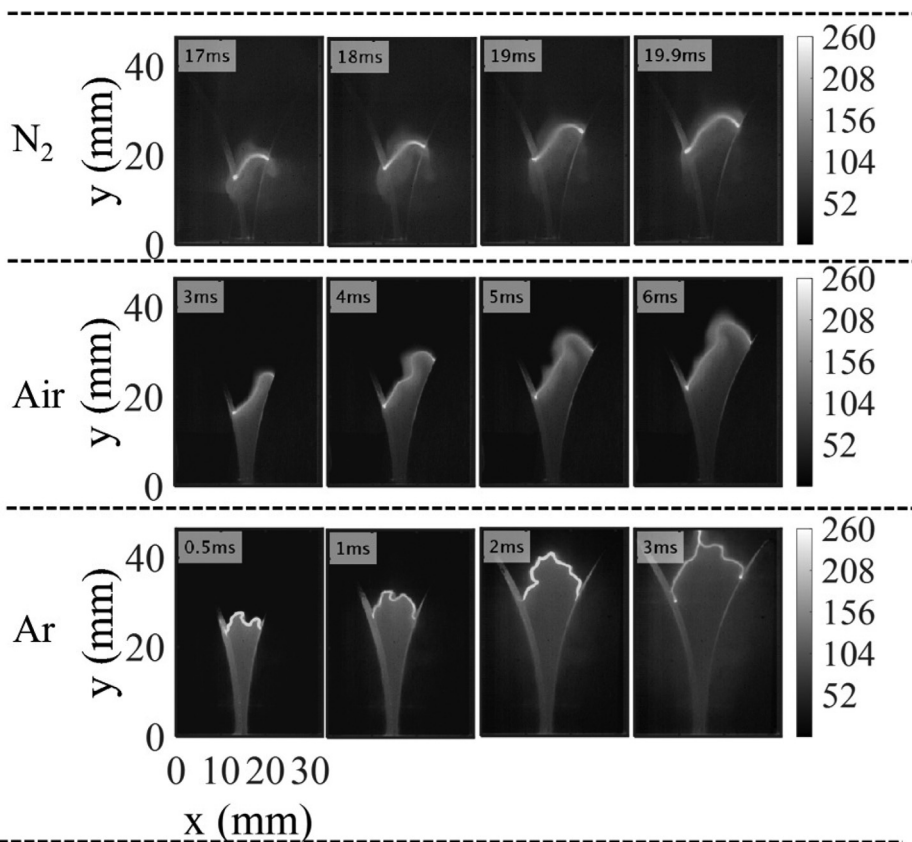
FIG. 7. Morphologies of plasma columns in different gas mixtures captured by a high-speed camera.

decreases to limit the current. Different from the air and N_2 plasmas, the Ar plasma column has a slightly increased E. Since the current amplitude is nearly constant with the pressure elevated from 1 to 5 atm in Ar, it is speculated that the electron density should be not sensitive to pressure.

IV. DISCUSSION

A. The glow-to-spark transition during the gliding arc discharge

For the conventional GAD, the voltage drop between electrodes (U) must be less than that for breakdown of fresh gas at the minimum gap between electrodes, i.e., Requirement (1) expressed as below:

$$U < E_{bk} \times l_{min}, \qquad (1)$$
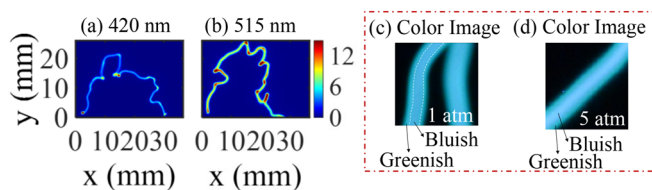
FIG. 8. Imaging of plasma columns in the Ar-0.1%CH$_4$ mixture. (a) and (b) are captured by the ICCD camera with a gate width of 30 μs; (c) and (d) are color images captured by the Nikon digital camera with an exposure time of 1/8000 s.
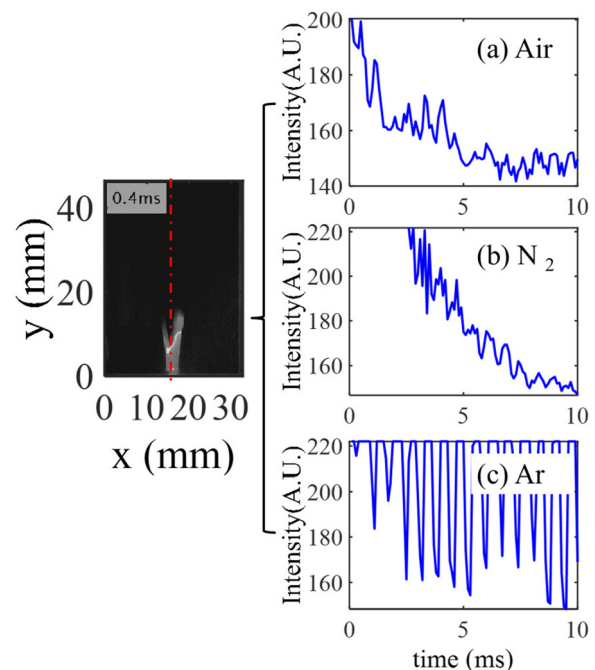
FIG. 9. Variations of the peak emission intensity of the plasma column over time when the plasma moves upward. The saturated value of intensity is set to 222.
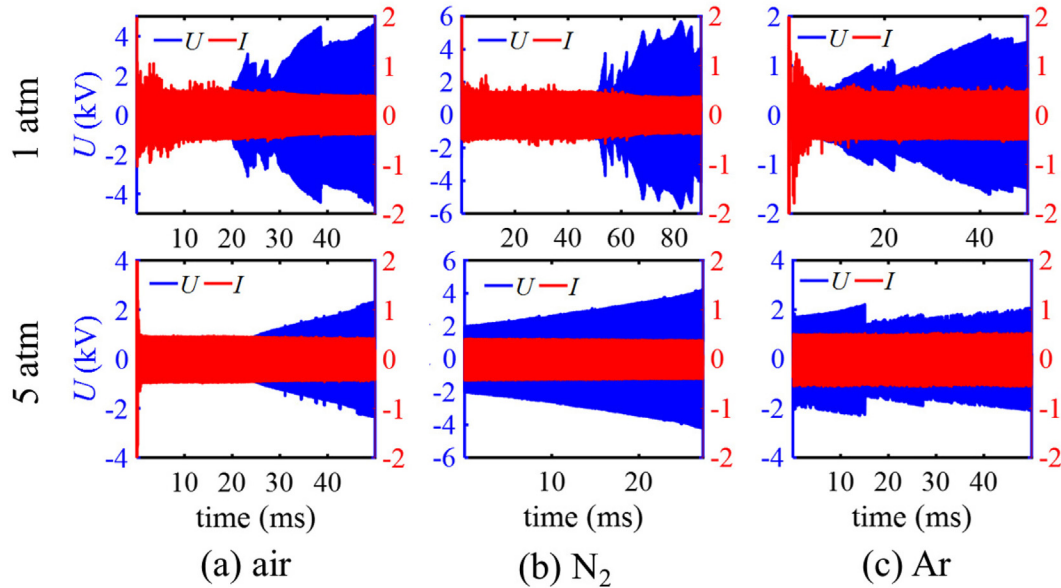
FIG. 10. I–U waveforms of GAD in the air, N_2 and Ar at the pressures of 1 and 5 atm.
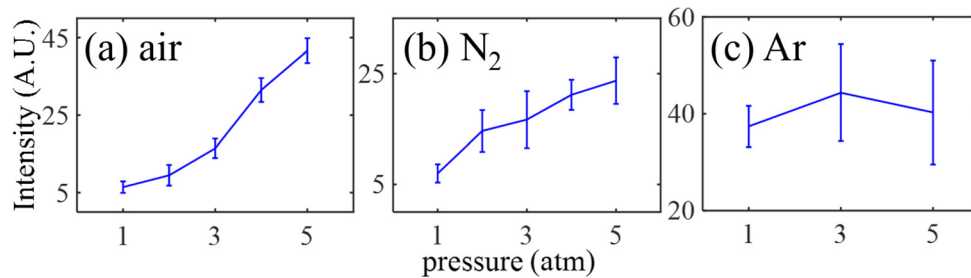
FIG. 11. Emission intensity of the plasma column with respect to pressure in the air, N_2, and Ar, respectively.

where E_{bk} is the electric field strength of breakdown in the fresh gas and l_{min} is the minimum gap distance between electrodes. Furthermore, the spark-type discharge occurs when the electric field strength is larger than that of breakdown along the plasma column (E_{sp}), i.e., Requirement (2), which can be expressed as follows:

FIG. 12. Images of the plasma column at 1 and 5 atm in (a) air, (b) N_2, and (c) Ar.

$$E_{sp} < \frac{U - U_{dp}}{l_{arc}}, \tag{2}$$

where l_{arc} is the length of the plasma column and U_{dp} denotes the effective voltage drop near the electrodes of the glow discharge. The glow-type discharge is sustained when the voltage (U) is less than $E_{sp} \times l_{arc}$. It indicates that the output voltage from the power supply is vital for the discharge mode control.

In this work, the gliding arc discharge system, including the power supply, the electrodes, the connecting cables, and the generated plasma, can be equivalent to an electrical circuit as shown in the inset of Fig. 1. The output voltage and current from the power supply vary from case to case and can be treated as a black box with some presumed characteristics for simplicity. Here, the output voltage from the AC power supply (U_0) is assumed to have a sinusoidal waveform, given by

$$U_0(t) = V_0 \cos(2\pi f t), \tag{3}$$

where t denotes time, f is the frequency of alternating voltage, and V_0 is the amplitude of alternating voltage, which can change with the

FIG. 13. Voltage amplitude-plasma column length curves of the GAD in air, N$_2$, and Ar at pressures of 1, 3, and 5 atm.

current amplitude. The coaxial cable, which connects the power supply and the electrodes, has the equivalent capacitance (C$_1$) and resistance (R$_1$). The electrodes can be treated as a switch to have an equivalent capacitance (C$_2$) and a resistance (R$_2$). When the plasma is formed, the switch is on and the plasma is regarded as a resistance (R$_2$) to connect the two electrodes. Note that for the glow-type discharge, a voltage drop near the electrodes always occurs. Here, it is considered as a nearly constant voltage drop (U$_{dp}$). When no plasma is formed, R$_2$ is assumed to be infinite. According to the configurations and sizes of the electrodes and the coaxial cable, the capacitance between electrodes (C$_2 < 1$ pF) is estimated to be much smaller than C$_1$ ($\sim$100 pF) and, thus, it is neglected. Furthermore, Fig. 4(a) has indicated that the phase shift between current and voltage waveforms is small during the glow-type discharge. It means that the impacts from C$_1$ can be neglected during the glow-type discharge. As a result, when the glow-type discharge is formed, the current (I$_2$) and the voltage (U$_2$) between the electrodes are derived to be expressed as follows:

$$I_2(t) = \frac{V_0[\cos(2\pi f t)] - U_{dp}}{R_1 + R_2}, \qquad (4)$$

$$U_2(t) = I_2(t) \times R_2 + U_{dp}. \qquad (5)$$

For the glow-type GAD, the plasma column can be treated as a conductive load, whose impedance is mainly governed by the instantaneous n$_e$. Hence, R$_2$ is directly related to the free electron density, n$_e$, expressed as

$$R_2 = l_{arc}/(\pi r^2 e n_e \mu_e), \qquad (6)$$

where r is the radius of the plasma column, e is the elementary electron charge, n$_e$ is the free electron density, and μ_e is the electron mobility.

Combining the expressions (2), (4), (5), and (6), Requirement (2) for the repetitive spark discharge is derived as follows:

$$E_{sp} < \frac{V_0\cos(2\pi f t) - U_{dp}}{[l_{arc} + R_1\pi r^2 e n_e \mu_e]}. \qquad (7)$$

The glow-to-spark transition occurs when the electric field strength in the plasma column is larger than E$_{sp}$. According to inequation (7), spark is more likely to occur as V$_0$ is larger while l_{arc} and n$_e$ becomes smaller. We further find that a fast decay of free electron density in the plasma column is beneficial to meet Requirement 2 since it can result in higher V$_0$, shorter l_{arc}, and smaller n$_e$, all of which can increase the internal electric field strength to trigger sparks. The characteristic decay time of free electron depends on gas compositions and temperatures, which are also functions of the flow field. Therefore, when the power supply is given, the discharge characteristics can be modified by the flow condition and the gas compositions. As found in the previous experiment,[16,17] when the flow rate is extremely high to produce intense turbulence, the gas temperature is lower due to strong energy dissipation and, thus, n$_e$ decays rapidly to trigger spark discharges.[33] In the Ar GAD, with the addition of O$_2$, the electron density

FIG. 14. I–U waveforms with different delay times (a) 84, (b) 336, and (c) 280 μs.

drops fast due to the attachment by O_2. It, thereby, results in a higher voltage from the power supply to trigger spark discharges.

At a deeper level, we can speculate that the GAD mode is essentially determined by the interactions of the produced plasma and the power supply. For a given power supply, the changes in the gas composition or the flow rate can modify the plasma states to influence the discharge mode. On the other hand, regulating the power supply characteristics can induce different discharge modes as well if the gas composition or the flow rate is given. As a test, the delay time between high-voltage (HV) bursts from the power supply was modulated by a pulse generator (BNC 575). With the delay time increase, n_e decreases and V_0 increases when the next HV burst starts.[33] As the delay time is raised to 336 μs at a flow rate of 10 SLPM or 280 μs at a flow rate of 20 SLPM, sparks along the plasma column occur, as shown in Fig. 14. It confirms that modulating the power supply can efficiently control the instant plasma states as well as the discharge modes. Therefore, for practical applications, power supply design and optimization should be necessary to regulate the GAD characteristics.

B. Gas-dependent pressure effects on the NE-GAD characteristics

The experimental results show that the pressure effects on the GAD vary with gas compositions. For instance, in Ar, E increases slightly with pressure and the emission intensity is nearly constant, while in air and N_2, E decreases and the emission intensity becomes much stronger with pressure. This distinction can be ascribed to the gas-dependent energy partition and energy transfer pathways. Figure 15 presents a schematic of the main chemical reaction pathways in Ar, N_2, and air plasma, respectively, that can be used to interpret the energy transfer pathways.

In Ar, the GAD is a glow-type discharge when the pressure elevates up to 5 atm. For the glow GAD, the electron density (n_e) varies relatively slow with time and its value is close to $n_{e,0}$, which is the electron density under the local equilibrium approximation and can be formulated by a function of the translational temperature (T_g), the vibrational temperature (T_v), the electronic temperature (T_{exe}), and the gas compositions ($[X]$), expressed by

$$n_{e,0} = f\left(T_g, T_v, T_{exe}, [X]\right). \qquad (8)$$

It means that n_e is not dependent on the alternating voltage directly and mainly determined by the thermal states of plasma. Meanwhile, it

has been found that the current amplitude is near 0.5 A and the electric field strength, E, is around 8 kV/m as the pressure increases. Therefore, the input power density does not change much with pressure in the argon. The heat conductivity of argon is nearly constant with pressure from 1 to 5 atm, so the gas temperature in the plasma column is insensitive to pressure. It, thereby, infers that with pressure increase, the thermal state does not change much and so is n_e. On the contrary, the electronic excitation of argon is governed by the local E/N since the emission from the plasma column has been found to fluctuate with the alternating voltage. As the pressure increases and E does not increase much, E/N drops and, thus, the emission intensity cannot increase with pressure.

For the glow-type N_2 or air GAD, the net electron production rate and the electronic excitation process are both insensitive to the alternating voltage according to the experiment. It thus supports the proposed energy partition and transfer pathways in Fig. 15. N_2 and O_2 are molecules to be mostly vibrationally excited by energetic electrons in the glow-type plasma since the electron temperature is not high enough for electronic excitation or ionization directly. Those vibrationally excited molecules can further produce the electronically excited species and even electrons through ladder excitation processes.[34,35] According to the proposed chemical reaction pathways in Fig. 15, with pressure and molecular number density increase, the collision frequency is higher to produce more vibrationally excited

FIG. 15. Schematic of the chemical reaction pathways in the (a) Ar, (b) N_2, and (c) air plasma.

species, which further result in more electronically excited species and electrons. In N_2 plasma, $N_2(A)$, $N_2(B)$, $N_2(C)$, $N_2(B)^+$, and electron can be effectively produced with the help of vibrationally excited $N_2(v)$, whereas in air, atomic N and O can be efficiently produced to form $NO(B)$ and NO^+, which have been detected from the spectra. As n_e increases, the power supply has feedback response to reduce voltage and E.

V. CONCLUSIONS

This work investigates the effects of gas compositions and pressures on the NE-GAD characteristics by electrical and optical methods. The main conclusions are listed as follows:

(1) The glow-to-spark transition can be modulated by different ways, such as changing the gas compositions, increasing the flow rate, and prolonging the inter-burst delay time of the output voltage of the power supply. The effective electron decay time in the produced plasma column is a key factor to impact the discharge mode. Short decay time of electrons can result in the spark-type discharge more easily. Meanwhile, the response of the power supply to the free electron density is also crucial. Modulating the power supply is an efficient way to control the discharge mode when the gas composition and the flow conditions have been given.

(2) Pressure effects on the GAD characteristics change depending on the specific gas. In N_2 and air, the emission intensity from the plasma column increases and the electric field strength decreases as the pressure elevates. In Ar, the emission intensity and E are insensitive to pressure. The reason is attributed to the different energy transfer and excitation/ionization pathways. Argon is atomic species, and thus, the electronic excitation process is governed by E/N, while N_2 and air are molecular species, and the input electric energy is largely transferred through vibrational excitation pathways in the glow-type GAD. The produced vibrationally excited species can further produce electronically excited species, atomic species, and electrons to sustain the plasma. Elevated pressure promotes the collisional excitations between vibrationally excited species to result in stronger light emission and higher electron density in N_2 and air.

ACKNOWLEDGMENTS

AUTHOR DECLARATIONS

Conflict of Interest

The authors have no conflicts of interest to disclose.

DATA AVAILABILITY

The data that support the findings of this study are available within the article.

REFERENCES

[1]A. Fridman, S. Nester, L. A. Kennedy, A. Saveliev, and O. Mutaf-Yardimci, Prog. Energy Combust. Sci. **25**, 211–231 (1999).
[2]H. Lesueur, A. Czernichowski, and J. Chapelle, J. Phys. Colloques **51**, C5-57–C5-64 (1990).
[3]A. Fridman, *Plasma Chemistry* (Cambridge, 2008).
[4]J. Liu, X. Li, J. Liu, and A. Zhu, Plasma Sources Sci. Technol. **29**, 015022 (2020).
[5]Y. Ju and W. Sun, Prog. Energy Combust. Sci. **48**, 21–83 (2015).
[6]K. Li, J. Liu, X. Li, X. Zhu, and A. Zhu, Chem. Eng. J. **288**, 671–679 (2016).
[7]J. Liu, X. Li, J. Liu, and A. Zhu, J. Phys. D: Appl. Phys. **52**, 284001 (2019).
[8]J. Pacheco, R. Valdivia, M. Pacheco, and A. Clemente, Int. J. Hydrogen Energy **45**, 31243–31254 (2020).
[9]J. Gao, C. Kong, J. Zhu, A. Ehn, T. Hurtig, Y. Tang, S. Chen, M. Alden, and Z. Li, Proc. Combust. Inst. **37**, 5629–5636 (2019).
[10]Y. D. Korolev, O. B. Frants, N. V. Landl, V. G. Geyman, and I. B. Matveev, IEEE Trans. Plasma Sci. **35**, 1651–1657 (2007).
[11]W. Wang, D. Mei, X. Tu, and A. Bogaerts, Chem. Eng. J. **330**, 11–25 (2017).
[12]L. Yu, X. Li, X. Tu, Y. Wang, S. Lu, and J. Yan, J. Phys. Chem. A **114**, 360–368 (2010).
[13]F. Zhu, X. Li, H. Zhang, A. Wu, J. Yan, M. Ni, H. Zhang, and A. Buekens, Fuel **176**, 78–85 (2016).
[14]H. Zhang, F. Zhu, X. Li, and C. Du, Plasma Sci. Technol. **19**, 045401 (2017).
[15]F. Mitsugi, T. Ohshima, H. Kawasaki, T. Kawasaki, S. I. Aoqui, T. Baba, and S. Kinouchi, IEEE Trans. Plasma Sci. **42**, 3681–3686 (2014).
[16]J. Zhu, J. Gao, A. Ehn, M. Alden, A. Larsson, Y. Kusano, and Z. Li, Phys. Plasmas **24**, 013514 (2017).
[17]C. Kong, J. Gao, J. Zhu, A. Ehn, M. Alden, and Z. Li, J. Appl. Phys. **123**, 223302 (2018).
[18]C. Kong, J. Gao, J. Zhu, A. Ehn, M. Alden, and Z. Li, Phys. Plasmas **24**, 093515 (2017).
[19]F. Zhu, H. Zhang, X. Li, A. Wu, J. Yan, M. Ni, and X. Tu, J. Phys. D: Appl. Phys. **51**, 105202 (2018).
[20]T. Zhao, J. Liu, X. Li, J. Liu, Y. Song, Y. Xu, and A. Zhu, Phys. Plasmas **21**, 053507 (2014).
[21]H. Zhang, C. Du, A. Wu, Z. Bo, J. Yan, and X. Li, Int. J. Hydrogen Energy **39**, 12620–12635 (2014).
[22]S. P. Gangoli, A. F. Gutsol, and A. A. Fridman, Plasma Sources Sci. Technol. **19**, 065003 (2010).
[23]N. Balcon, N. Benard, P. Braud, A. Mizuno, G. Touchard, and F. Moreau, J. Phys. D: Appl. Phys. **41**, 205204 (2008).
[24]L. Potocnakova, J. Sperka, P. Zikan, J. J. W. A. van Loon, J. Beckers, and V. Kudrle, Plasma Sources Sci. Technol. **24**, 022002 (2015).
[25]J. Sperka, P. Soucek, J. J. W. A. van Loon, A. Dowson, C. Schwarz, J. Krause, G. Kroesen, and V. Kudrle, Eur. Phys. J. D **67**, 261 (2013).
[26]J. Ananthanarasimhan, R. Lakshminarayana, M. S. Anand, and S. Dasappa, Plasma Sources Sci. Technol. **28**, 085012 (2019).
[27]J. Diatczyk, G. Komarzyniec, and H. D. Stryczewska, Int. J. Plasma Environ. Sci. Technol. **5**, 12–16 (2011).
[28]N. C. Roy and M. R. Talukder, Phys. Plasmas **25**, 093502 (2018).
[29]P. G. Rutberg, A. A. Safronov, and V. L. Goryachev, IEEE Trans. Plasma Sci. **26**, 1297–1306 (1998).
[30]C. Kong, J. Gao, Z. Li, M. Alden, and A. Ehn, Appl. Phys. Lett. **114**, 194102 (2019).
[31]P. H. Joo, J. Gao, Z. Li, and M. Alden, Rev. Sci. Instrum. **86**, 035115 (2015).
[32]C. O. Laux, T. G. Spence, C. H. Kruger, and R. N. Zare, Plasma Sources Sci. Technol. **12**, 125–138 (2003).
[33]C. Kong, J. Gao, J. Zhu, A. Ehn, M. Alden, and Z. Li, Appl. Phys. Lett. **112**, 264101 (2018).
[34]M. Capitelli, G. Colonna, G. D'Ammando, V. Laporta, and A. Laricchiuta, Chem. Phys. **438**, 31–36 (2014).
[35]J. Annaloro and A. Bultel, J. Thermophys. Heat Transfer **28**, 608–622 (2014).